Dalton Transactions

PAPER

View Article Online
View Journal | View Issue

Published on 17 January 2014. Downloaded by National Chung Hsing University on 02/04/2014 15:44:44.

Cite this: *Dalton Trans.*, 2014, **43**, 5200

Magnesium complexes containing biphenyl-based tridentate imino-phenolate ligands for ring-opening polymerization of *rac*-lactide and α-methyltrimethylene carbonate†

Wei Yi and Haiyan Ma*

Received 14th December 2013,
Accepted 15th January 2014

DOI: 10.1039/c3dt53513d

www.rsc.org/dalton

A series of racemic 2-[(2′-(dimethylamino)biphenyl-2-ylimino)methyl]-4-R^2-6-R^1-phenols (**L^1H–L^4H**) were reacted with $\{Mg[N(SiMe_3)_2]_2\}_2$ to provide four heteroleptic magnesium complexes (**L^{1-4}**)MgN-$(SiMe_3)_2$·$(THF)_n$ (**1**, R^1 = ^{t}Bu, R^2 = Me, n = 1; **2**, R^1 = R^2 = CMe_2Ph, n = 0; **3**, R^1 = CPh_3, R^2 = ^{t}Bu, n = 1; **4**, R^1 = Br, R^2 = ^{t}Bu, n = 0), which have been fully characterized. X-ray structural determination shows that complex **1** possesses a monomeric structure, but complex **4** is dimeric with C_2-symmetry where the two metal centers are bridged by two phenolate oxygen atoms of the ligands. The coordination geometry around the magnesium center in these complexes can be best described as a distorted tetrahedral geometry. The heteroleptic complexes **1–4** efficiently initiate the ring-opening polymerization of *rac*-lactide and α-methyltrimethylene carbonate (α-MeTMC) and the polymerizations are better controlled in the presence of 2-propanol. In general, the introduction of a bulky *ortho*-substituent on the phenoxy unit results in increases of both the catalytic activity and the stereo- or regioselectivity of the corresponding magnesium complex. Microstructure analyses of the resulting PLAs revealed that P_r values range from 0.46 to 0.81, depending on the catalyst and the polymerization conditions. For racemic α-MeTMC, detailed analyses using ^{1}H and ^{13}C NMR spectroscopy indicated the preferential ring-opening of α-MeTMC at the most hindered oxygen–acyl bond (X_{reg} = 0.65–0.86).

Introduction

Biodegradable aliphatic polyesters and polycarbonates such as poly(lactic acid) (PLA) and poly(α-methyltrimethylene carbonate) (P(α-MeTMC)) have received increased interest in recent years, which is largely due to the biodegradability and biocompatibility of the resulting materials as well as their versatile chain microstructures derived from the selective ring-opening polymerization (ROP) process of related cyclic monomers in racemic form.[1–4] Since the microstructure of the monomeric units in the polymer chain plays a decisive role in determining mechanical and physical properties of the polymeric materials, the design and synthesis of well-defined metal catalysts to prepare PLA or P(α-MeTMC) of specific architectures have become a major topic.[5,6]

In the past two decades, a variety of well-characterized metal complexes capable of initiating the ROP of lactides have been reported.[7–42] Among these numerous metal-based catalysts that have been disclosed for polymerization studies, complexes of biocompatible metals such as Groups 1[15–18] and 2[26–31] metals as well as zinc[19–24] are preferable to be used. In the complexes, the structure of the ancillary ligand proves to play an important role in the stereo-chemistry of resulting polymers. Discrete Mg and Zn complexes with β-diketiminate ligands show high activity and heterotactic selectivity for the ring-opening polymerization of *rac*-lactide.[43–46] Lin and co-workers[47] reported a series of zinc complexes bearing NNO-tridentate iminophenolate ligands which initiate *rac*-lactide polymerization to afford heterotactic PLA (P_r = 0.59–0.74) at 25 °C. Darensbourg's group[48] introduced zinc silylamido complexes supported by chiral NNO-tridentate iminophenolate ligands for the polymerization of *rac*-lactide in dichloromethane to afford heterotactic predominant PLA (P_r = 0.68 to 0.89).

Shanghai Key Laboratory of Functional Materials Chemistry and Laboratory of Organometallic Chemistry, East China University of Science and Technology, 130 Meilong Road, Shanghai 200237, People's Republic of China.
E-mail: haiyanma@ecust.edu.cn; Fax: +86 21 64253519; Tel: +86 21 64253519

†Electronic supplementary information (ESI) available: A comparison of dimethylamino proton chemical shifts of complexes and proligands, ^{1}H NMR trace spectra of the reaction between **2** and 2-propanol, ^{1}H NMR spectrum of PLA oligomer, homonuclear-decoupled ^{1}H NMR spectra of PLAs, ^{1}H NMR spectrum and ESI-TOF mass spectrum of poly(α-MeTMC) oligomer, DSC curves of poly(α-MeTMC) and X-ray crystallographic data of complexes **1** and **4** in CIF format. CCDC 973421 and 973422 for **1** and **4**. For ESI and crystallographic data in CIF or other electronic format see DOI: 10.1039/c3dt53513d

This journal is © The Royal Society of Chemistry 2014

Published on 17 January 2014. Downloaded by National Chung Hsing University on 02/04/2014 15:44:44.

Various types of metal-based catalysts[49–55] are also known to be efficient initiators for the ROP of trimethylene carbonate (TMC). Unfortunately, polymerizations of similar chiral cyclic carbonates, for instance, α-methyltrimethylene carbonate (α-MeTMC), have scarcely been explored. Rare earth alkoxides ("Ln(O^iPr)$_3$", Ln(OAr)$_3$, Ar = 2,6-di-*tert*-butyl-4-methylphenolate; Ln = La, Dy, Y) were revisited recently for the polymerization of this monomer; polycarbonates of high molar mass (M_n up to 30 000 g mol^{-1}) and relatively narrow molar mass distribution values ($1.1 < M_w/M_n < 1.7$) were obtained.[56] Guillaume and co-workers[57] used [(BDI^{iPr})Zn(N(SiMe$_3$)$_2$)] and Al(OTf)$_3$ to initiate the ROP of α-MeTMC respectively. The β-diketiminate zinc catalyst can obtain 94% monomer conversion within 7 min in toluene at 60 °C, but the Al(OTf)$_3$/BnOH system is only active at a high temperature of 110 °C. Meanwhile the zinc complex is highly regioselective ($X_{reg} > 0.98$) and prefers to ring-open the more sterically hindered O–C(O) bond. Compared to the extensive studies on *rac*-lactide polymerization, the catalyst systems involved in α-MeTMC polymerization are rather limited.

Very recently, we reported that a series of magnesium silylamido complexes supported by racemic methoxybiphenyl-based iminophenolate ligands exhibit moderate activities and heterotactic selectivities for the polymerization of *rac*-lactide.[58] Possibly due to the rigidity of the biphenyl skeleton, the methoxy group is dissociated from the metal center with the addition of a donating solvent or monomer, which is suggested to weaken the chiral induction effect of the biphenyl moiety and lead to a heteroselectivity instead of the desired isoselectivity. To further understand the effect of the ligand framework on the selective polymerization of *rac*-LA and α-MeTMC, we report herein a series of magnesium complexes supported by tridentate iminophenolate ligands based on the racemic dimethylaminobiphenyl framework. The catalytic performance of these silylamido complexes towards the ROP of *rac*-lactide and α-MeTMC are studied in detail.

Results and discussion

Synthesis and characterization of magnesium complexes

Scheme 1 illustrates the synthetic strategies to prepare the desired dimethylaminobiphenyl-based iminophenol proligands. 2,2′-Dinitrobiphenyl was synthesized *via* an Ullmann coupling reaction of 1-iodo-2-nitrobenzene.[59] The selective reduction of one nitro group using an ethanol solution of NaS_x afforded 2-amine-2′-nitrobiphenyl in a moderate yield of 50%.[60] 2-Dimethylamino-2′-aminobiphenyl was then obtained in high yield *via* an *N*-methylation of 2-amine-2′-nitrobiphenyl followed by a reduction with tin as the reducing agent. Condensation reactions of this amine with different salicylaldehyde derivatives under reflux in ethanol yielded the target dimethylaminobiphenyl-based iminophenol proligands **L$^{1–4}$H**. All the obtained iminophenols are yellow to orange crystalline solids which have been well-characterized *via* ^{1}H and ^{13}C{^{1}H} NMR spectroscopy and HRMS.

The heteroleptic magnesium complexes **1–4** were prepared in moderate yields from the reaction of {Mg[N(SiMe$_3$)$_2$]$_2$}$_2$ with one equivalent of the corresponding proligand in toluene at room temperature, respectively (Scheme 2). Analytically pure complexes **1** and **3** were successfully obtained *via* recrystallization with a THF–*n*-hexane mixture at −38 °C as yellow green crystalline solids, where the coordination of one THF molecule to the magnesium center was characterized spectroscopically. Complexes **2** and **4** were recrystallized with a toluene–*n*-hexane mixture at −38 °C and isolated as yellow green crystalline solids. Although there are both axial chirality of the biphenyl moiety and a stereogenic metal center in these complexes, no diastereomer could be observed in the ^{1}H NMR spectra, suggesting that the axial chirality of biphenyl may have induced exclusively a certain configuration around the magnesium center. As indicated in Fig. 1 and 2, in the solid state, complexes **1–3** are monomeric, while complex **4** possesses a dimeric structure. These structural features are however

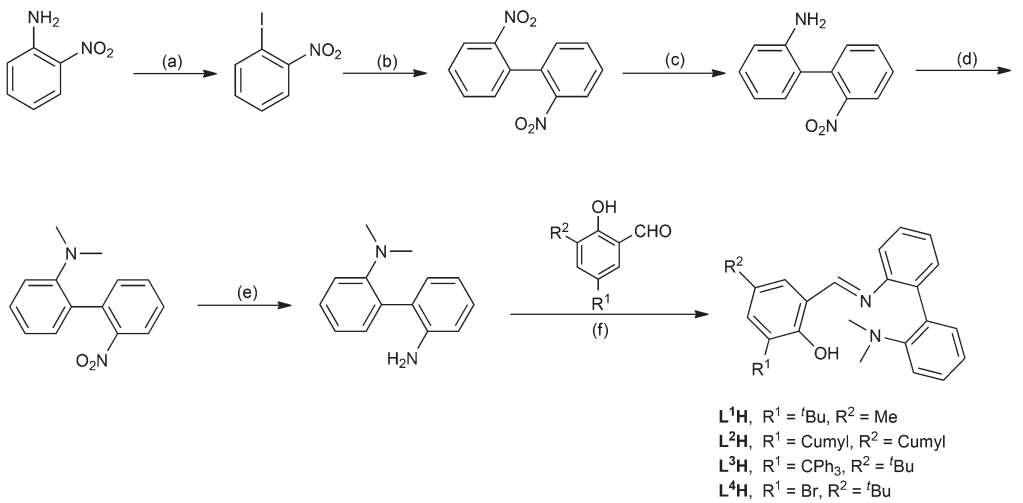

Scheme 1 Synthesis of proligand **L^{1}H–L^{4}H**[a]. (a) −5 to 0 °C, HCl/$NaNO_2$/KI. (b) Cu, 60 °C, under argon. (c) NaS_x, ethanol, reflux 6 h. (d) 40% HCHO, 20% H_2SO_4, $NaBH_4$, THF, −5 to 5 °C. (e) Sn/HCl, ethanol, reflux 5 h. (f) ethanol, reflux.

Published on 17 January 2014. Downloaded by National Chung Hsing University on 02/04/2014 15:44:44.

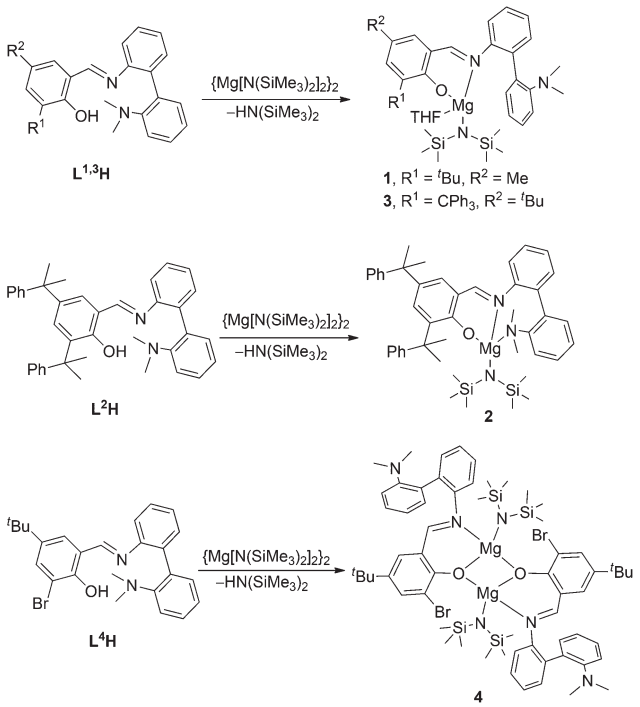

Scheme 2 Synthesis of magnesium complexes **1**–**4**.

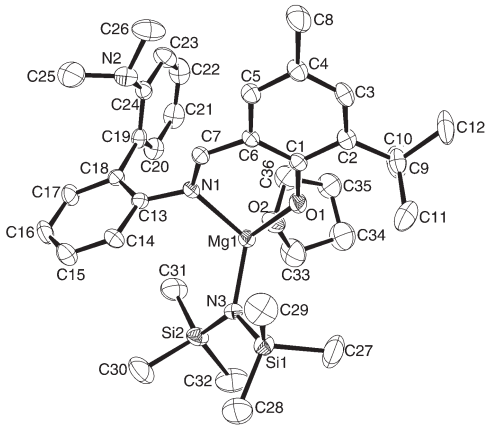

Fig. 1 ORTEP diagram of complex **1** (thermal ellipsoids drawn at 30% probability level). Selected bond lengths (Å) and angles (°): Mg1–O1 1.907(4), Mg1–O2 2.036(4), Mg1–N3 1.986(4), Mg1–N1 2.101(4), O1–Mg1–N3 126.0(2), O1–Mg1–O2 95.29(17), N3–Mg1–O2 109.19(19), O1–Mg1–N1 90.23(16), N3–Mg1–N1 117.44(17).

similar to the previously reported magnesium complexes ligated by methoxybiphenyl-based iminophenolate ligands.[58]

The stoichiometric structures of complexes **1**–**4** were further confirmed on the basis of ^{1}H and ^{13}C{^{1}H} NMR spectroscopy as well as elemental analysis. The ^{1}H NMR spectrum of **1** in benzene-d_6 shows one set of resonances of THF protons at 3.34 and 1.21 ppm, and one singlet assignable to $N(SiMe_3)_2$ protons at 0.31 ppm as well as one set of signals for the multidentate iminophenolate ligand, consistent with the stoichiometric structure illustrated in Scheme 2. The sharp signal at

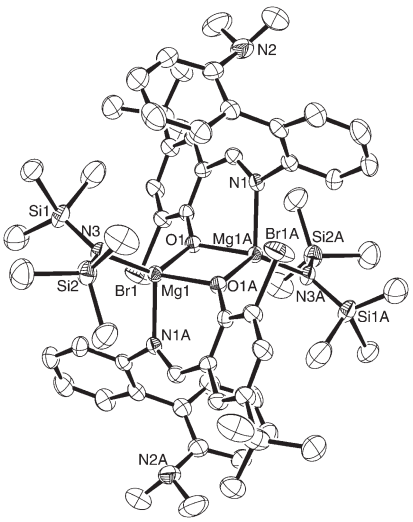

Fig. 2 ORTEP diagram of complex **4** (thermal ellipsoids drawn at 30% probability level). Selected bond lengths (Å) and angles (°): Mg1–O1 1.996(3), Mg1–O1A 2.026(3), Mg1–N3 2.004(4), Mg1–N1A 2.159(4), Mg1···Mg1A 3.076(3), Mg1···Br1 3.803, O1–Mg1–N3 131.02(17), O1–Mg1–O1A 80.22(13), O1–Mg1–N1A 109.66(14), N3–Mg1–O1A 126.28(16), N3–Mg1–N1A 112.39(17).

2.22 ppm accounting for protons of the dimethylamino group indicates that this group is dissociated from the metal center. A similar phenomenon is also observed in the ^{1}H NMR spectrum of **3** in benzene-d_6 where the resonance of dimethylamino protons appears at 2.23 ppm, which is close to that of the free ligand $\mathbf{L^3H}$ (2.17 ppm). As for complex **2**, the relevant resonance appears at 2.22 ppm, which is also close to the corresponding signal of the free ligand $\mathbf{L^2H}$ in benzene-d_6, but broadened reasonably. We suggest that it is most likely due to the specific shielding effect of the aromatic ring of the cumyl group and in complex **2** the dimethylamino group is still coordinated to the metal center in solution. To prove this assumption, 3 equiv. of THF was added to the solution of complex **2** in benzene-d_6 and the mixture was checked with ^{1}H NMR spectroscopy. A sharp signal assignable to dimethylamino protons could be observed at 2.10 ppm which is slightly upfield shifted, indicating that the addition of THF leads to the dissociation of this dimethylamino group. Similar to our previous work,[58] two sets of signals accounting for the stoichiometric structure are displayed in the ^{1}H NMR spectrum of complex **4** in benzene-d_6, represented by the dimethylamino resonances at 2.55 and 2.36 ppm (with a ratio of 3 : 1). Although the X-ray diffraction determination indicates a dimeric structure of complex **4** in the solid state where the dimethylamino group of the biphenyl moiety is not coordinated to the magnesium center, a significant downfield shift of the dimethylamino resonance attributable to the major structure is also observed when compared to that of the free ligand. The relevant resonance of the minor structure however resembles the one of the free ligand. In the presence of added THF (around 3 equiv.), these two signals coalesce to a singlet at 2.09 ppm (Table S1†). Obviously, the structure of **4** in solution

 This journal is © The Royal Society of Chemistry 2014

Published on 17 January 2014. Downloaded by National Chung Hsing University on 02/04/2014 15:44:44.

is mainly monomeric where the dimethylamino group in the biphenyl fragment is coordinated to the metal center.[58]

Molecular structures of magnesium complexes

Complexes **1** and **4** were further characterized by single crystal X-ray diffraction. Complex **1** was obtained as needle crystals by slightly cooling a saturated tetrahydrofuran–*n*-hexane mixture and complex **4** was recrystallized as tabular crystals with a toluene–*n*-hexane mixture. Crystallographic data and results of the refinements are summarized in Table 1.

As shown in Fig. 1, complex **1** has a monomeric structure in the solid state in which the magnesium atom is four-coordinated by two heteroatom donors of the tridentate ligand, one bis(trimethylsilyl)amido group and one THF molecule adopting a distorted tetrahedral geometry. The molecule shows C_1-symmetry and both enantiomers are found in the centrosymmetric crystal structure. Without exception, the R_a-configuration of the biphenyl moiety of the iminophenolate ligand leads to the *R*-configuration of the magnesium center, and *vice versa* S_a leads to the *S*-configuration. The bond length of magnesium to silylamido nitrogen atom (Mg1–N1) in complex **1** is 1.986(4) Å, which is very similar to that we reported before.[58] The dihedral angle of the biphenyl moiety being 71.34°, obviously also similar to that we reported previously, is likely due to the dissociation state of the dimethylamino group from the magnesium center. The ORTEP drawing of the molecular structure of **4** given in Fig. 2 indicates that in the solid state, complex **4** possesses a dimeric structure with a Mg1/O1/Mg1A/O1A planar core bridged by the two phenolato oxygen atoms of the ligands and the whole molecule has C_2-symmetry. Each magnesium center adopts a distorted tetrahedral geometry. The dimethylamino groups of both iminophenolate ligands are not coordinated with the magnesium centers. In the dimeric structure magnesium centers are achiral and the biphenyl moieties of the two ligands possess opposite configuration. The dihedral angle of biphenyl in **4** is 87.28°, which is significantly larger than that of complex **1**. Being different from our previous work where the C_1-symmetric magnesium silylamido dimer with *ortho*-bromo substitution gives two different Mg···Br distances of 3.469 Å and 3.871 Å,[58] the distance between Mg1···Br1 (or Mg1A···Br1A) in **4** is 3.803 Å, clearly indicating that there is no clear interaction between the Mg center and the Br atom in this work.

Table 1 Crystallographic data for complexes **1** and **4**

	1	**4**
Formula	$C_{72}H_{110}Mg_2N_6O_4Si_4$	$C_{62}H_{88}Br_2Mg_2N_6O_2Si_4$
F_w	1284.64	1270.18
Temp. (K)	296(2)	296(2)
Crystal size (mm)	0.35 × 0.20 × 0.04	0.25 × 0.15 × 0.12
Crystal system	Monoclinic	Triclinic
Space group	$P2(1)/c$	$P\bar{1}$
a (Å)	9.638(4)	11.442(7)
b (Å)	23.829(10)	13.370(8)
c (Å)	17.341(7)	14.072(8)
α (°)	90	61.692(11)
β (°)	101.146(7)	87.288(12)
γ (°)	90	70.508(11)
Volume (Å^3)	3908(3)	1770.7(18)
Z	2	1
D_{calcd} (mg m^{-3})	1.092	1.191
Abs. coeff. (mm^{-1})	0.139	1.272
F (000)	1392	668
θ range (°)	1.47 to 25.05	1.66 to 26.00
Data collected (hkl)	±11, 0 to 28, 0 to 20	−14 to 13, ±16, −17 to 16
Reflns collected/unique	15 459/6976	12 709/6899
R_{int}	0.0558	0.0346
Max. and min. transmn	0.7456 and 0.4758	0.8623 and 0.7416
Data/restraints/para	6976/106/446	6899/222/435
Goodness-of-fit on F^2	0.994	1.039
Final R_1, wR_2 [$I > 2\sigma(I)$]	0.0813, 0.2012	0.0659, 0.1978
R_1, wR_2 (all data)	0.1520, 0.2494	0.1174, 0.2472
$\Delta\rho_{max,\ min}$/e Å^{-3}	0.298 and −0.374	0.761 and −0.865

Ring-opening polymerization of *rac*-lactide by complexes 1–4

As can be seen from the data compiled in Table 2, all of these magnesium complexes can effectively initiate the *rac*-lactide polymerization in THF at room temperature or in toluene at 70 °C. The polymers produced in either solvent have high molecular weights and relatively broad molecular weight distributions (M_w/M_n = 1.12–1.66).

To examine the influence of this type of dimethylaminobiphenyl-based iminophenolate ligand on the catalytic performance of the corresponding magnesium complexes, the polymerization behaviors of complexes **1–4** with different R^1, R^2 groups for *rac*-lactide polymerization were examined in detail. It is found that the presence of substituents, particularly the one at the *ortho*-position of the phenoxide unit, plays an important role in determining the polymerization activity. For example, using complex **2** bearing an *ortho*-cumyl substituent as the initiator, a monomer conversion of 88% could be obtained within 15 min at room temperature (Run 5). Complex **3** with a sterically bulky trityl group shows much higher activity which gives 94% conversion within 2 min under otherwise the same conditions (Run 9). Complex **1** with less sterically hindered *tert*-butyl group is found to be less active than complexes **2** and **3**. As observed for most of the systems reported,[33,61] the presence of a sterically bulky substituent at the *ortho*-position of the anionic atom is beneficial to the catalytic activity, likely due to the fact that the sterically bulky group might efficiently prevent the active centre from aggregation.[62]

Besides, the introduction of an electron-withdrawing Br group on the *ortho*-position of the phenoxide unit decreases the activity of magnesium complex **4**, which exhibits the lowest catalytic activity for *rac*-lactide polymerization among these complexes. A similar phenomenon was also observed by Lin's group[61,63] that magnesium benzyl alkoxide complexes [LMg-(μ-OBn)]$_2$ (L = NNO-tridentate iminophenolate[61] or β-ketiminato ligands[63]) with an electron-donating group on the ligand framework displayed high reactivity, while the reactivity decreased substantially with the substitution of an electron-withdrawing group. It is also in accord with the results of aluminium complexes reported by our group[64] and Tolman's group.[65]

Published on 17 January 2014. Downloaded by National Chung Hsing University on 02/04/2014 15:44:44.

Table 2 Ring-opening polymerization of *rac*-lactide initiated by magnesium silylamido complexes **1–4**[a]

Run	Initiator	$[LA]_0/[Mg]_0/[^iPrOH]_0$	Solvent	T (°C)	t (min)	Conv.[b] (%)	$M_{n,calcd}$[c] ($\times 10^4$)	M_n[d] ($\times 10^4$)	M_w/M_n[d]	P_r[e]
1	**1**	200 : 1 : 0	THF	25	30	90	2.59	3.49	1.53	0.69
2		200 : 1 : 1	THF	25	60	96	2.77	2.65	1.27	0.67
3		200 : 1 : 0	Tol	70	180	94	2.71	3.67	1.47	0.49
4		200 : 1 : 1	Tol	70	60	98	2.82	2.73	1.42	0.49
5	**2**	200 : 1 : 0	THF	25	15	88	2.54	3.82	1.63	0.72
6		200 : 1 : 1	THF	25	30	96	2.77	2.53	1.28	0.70
7		200 : 1 : 0	Tol	70	180	94	2.71	3.70	1.48	0.51
8		200 : 1 : 1	Tol	70	30	98	2.82	3.57	1.39	0.49
9	**3**	200 : 1 : 0	THF	25	2	94	2.71	13.7	1.51	0.77
10		200 : 1 : 0	THF	−38	2d	73	2.10	1.56	1.55	0.81
11		200 : 1 : 1	THF	25	30	98	2.82	2.95	1.31	0.71
12		200 : 1 : 0	Tol	70	120	93	2.68	3.64	1.40	0.48
13		200 : 1 : 1	Tol	70	20	98	2.82	2.82	1.66	0.46
14	**4**	200 : 1 : 0	THF	25	30	88	2.54	4.75	1.66	0.71
15		200 : 1 : 1	THF	25	180	80	2.30	2.44	1.12	0.69
16		200 : 1 : 0	Tol	70	480	94	2.71	3.44	1.46	0.50
17		200 : 1 : 1	Tol	70	300	95	2.74	2.36	1.48	0.50

[a] $[rac\text{-LA}]_0$ = 1.0 M. [b] Determined by ^{1}H NMR spectroscopy. [c] $M_{n,calcd} = ([LA]_0/[Mg]_0) \times 144.13 \times$ conv.%; in the presence of ^{i}PrOH, $M_{n,calcd} = ([LA]_0/[^iPrOH]_0) \times 144.13 \times$ conv.% + 60. [d] Determined by GPC. [e] P_r is the probability of forming a new *r*-diad, determined by homonuclear decoupled ^{1}H NMR spectroscopy.

As shown in Table 2, the polymerization medium also plays an important role in influencing the polymerization, and THF is a better solvent than toluene. When complex **1** is used as an initiator, a monomer conversion up to 90% is achieved within 30 min in THF at room temperature (Run 1), whereas the reaction takes 180 min in toluene at 70 °C (Run 3). A similar phenomenon was also observed by Lin and co-workers.[61]

In general, metal silylamido complexes have been reported to be inferior initiators for the ROP of *rac*-lactide and afforded broadly distributed polymers.[62,66] Therefore, *rac*-lactide polymerization initiated with complexes **1–4** in the presence of 2-propanol was also investigated. Before conducting systematic polymerization studies, the NMR tube reaction of complex **2** with 2-propanol was monitored. The 1 : 1 ratio reaction generated the expected iminophenolato magnesium alkoxide "[L^2MgO^{i}Pr]" along with the release of free amine $HN(SiMe_3)_2$ (δ = 0.091 ppm, Fig. S1†), indicating adequate tolerance of the bonding between the tridentate ligand and the magnesium center toward protonic sources. As shown in Table 2, the polymerizations of *rac*-lactide initiated by complexes **1–4**/2-propanol are well-controlled, giving polymers with relatively narrower molecular weight distributions. The addition of 2-propanol has different influence on the polymerization conducted in THF or in toluene which is different from most previous results, but consistent with the regularity we reported previously.[58] In THF, the polymerizations of *rac*-lactide initiated by complexes **1–4** in the presence of 2-propanol are unusually slow when compared to those without the addition of 2-propanol, while the order in toluene is still consistent with the literature reports.[20,21] Using complex **1** as the initiator, the polymerization can reach 90% conversion within 30 min in THF (Run 1), whereas the yield is only 96% after 60 min (Run 2) when initiated by complex **1**/2-propanol under otherwise the same conditions. In toluene, a monomer conversion of 94% can be achieved by **1** in 180 min; the addition of 2-propanol significantly shortens the polymerization time to 60 min accompanied by a conversion of 98% (Runs 3, 4). It is thus suggested that although an alkoxide group is superior to an amide group in initiation, a coordinative solvent may bring a complicated effect during the polymerization by either facilitating the dissociation of the *in situ* formed dimeric metal alkoxide species or blocking the coordination site *via* competitive coordination to the metal center.

The initiation mechanism was elucidated by end-group analysis of a *rac*-LA oligomer sample, which was prepared by the reaction of complex **2** with *rac*-LA in a 1 : 20 molar ratio. The existence of both terminal groups could be confirmed according to the resonances at about 1.23, 5.03 ppm (for isopropoxy) and 1.48, 4.34 ppm (for HOC*H*(CH_3)CO–) *via* ^{1}H NMR spectroscopy (Fig. S2†). Meanwhile, no proton resonance of the ligand is observed in the ^{1}H NMR spectrum of the oligomer, which reveals that the biphenyl-based tridentate iminophenolate group is not involved in the polymerization process. Thus, the polymerization proceeds *via* a common "coordination–insertion" mechanism initiated by the *in situ* generated magnesium isopropoxide "LMg(O^{i}Pr)".

Microstructure analyses of PLAs were achieved through inspecting the methine region of homonuclear decoupled ^{1}H NMR spectra of the resulting polymers. This series of silylamido magnesium complexes give moderate heterotactic selectivity (P_r = 0.67–0.77) in THF, whereas mostly atactic PLAs (P_r = 0.50–0.46) are obtained in toluene. A similar trend of solvent effect on the selectivity was often reported in the literature. For instance, Chisholm and co-workers[67] recently reported magnesium complexes L′Mg^{n}Bu(THF) supported by β-diimine ligands which showed high heteroselectivity (P_r = 0.96) in THF. When the solvent was changed to toluene/dichloromethane, the selectivity decreased considerably to 0.87. Carpentier and co-workers[68] also reported dianionic alkoxy-amino-bisphenolate yttrium complexes as initiators in

 This journal is © The Royal Society of Chemistry 2014

Published on 17 January 2014. Downloaded by National Chung Hsing University on 02/04/2014 15:44:44.

Table 3 Ring-opening polymerization of α-MeTMC initiated by magnesium silylamido complexes **1–4**[a]

Run	Initiator	$[\alpha\text{-MeTMC}]_0/[Mg]_0/[^i\text{PrOH}]_0$	t (min)	Conv.[b] (%)	$M_{n,calcd}$[c] ($\times 10^4$)	M_n[d] ($\times 10^4$)	M_w/M_n[d]	X_{reg}[e]	T_g[f] (°C)
1	**1**	200 : 1 : 0	180	90	2.09	4.56	1.42	0.74	4.32
2		200 : 1 : 1	120	95	2.20	2.34	1.37		
3	**2**	200 : 1 : 0	120	90	2.09	6.09	1.61	0.85	4.01
4		200 : 1 : 1	60	90	2.09	3.07	1.44		
5	**3**	200 : 1 : 0	60	92	2.13	10.06	1.48	0.86	−7.58
6		200 : 1 : 1	30	93	2.16	3.07	1.44		
7	**4**	200 : 1 : 0	180	88	2.04	7.26	1.50	0.65	1.43
8		200 : 1 : 1	120	89	2.06	3.73	1.61		

[a] $[\alpha\text{-MeTMC}]_0$ = 1.0 M; in toluene, at 70 °C. [b] Determined by ^{1}H NMR spectroscopy. [c] $M_{n,calcd} = ([\alpha\text{-MeTMC}]_0/[Mg]_0) \times 116.05 \times$ conv.%; in the presence of ^{i}PrOH, $M_{n,calcd} = ([\alpha\text{-MeTMC}]_0/[^i\text{PrOH}]_0) \times 116.05 \times$ conv.% + 60. [d] Determined by GPC. [e] X_{reg} is the percentage of head-to-tail/tail-to-head linkages (**A** and **D**) in the polymer chain, determined by ^{13}C NMR spectroscopy. [f] Determined by DSC.

the ROP of *rac*-lactide which gave high heteroselectivity in THF whereas it showed no selectivity in toluene.

In comparison with the crucial effect of a solvent, the nature of ligand substituents has a slight impact on the stereoselectivity. Complex **3** with a sterically bulky trityl group at the *ortho*-position of the phenoxide unit displays the highest preference for heterotactic diad enchainment during the polymerization of *rac*-lactide (P_r = 0.77, in THF, Fig. S3†), while the other complexes including complex **4** with an *ortho*-bromo substitution exhibit quite similar heterotactic selectivities (P_r = 0.69–0.72, in THF). Furthermore, the P_r values of the resulting polymer samples vary slightly upon changing the temperature. Using complex **3** as the initiator, the P_r value increases to 0.81 as the polymerization temperature decreases to −38 °C (Run 10; Fig. S4†).

Generally, this series of magnesium complexes exhibits similar catalytic activity and heteroselectivity for the ROP of *rac*-lactide as those we reported previously,[58] implying that the replacement of the methoxy group with a dimethylamino group in the biphenyl moiety has not brought a noticeable influence on the coordination mode of the ligand as well as their steric and electronic features.

Ring-opening polymerization of α-MeTMC by complexes 1–4

The catalytic behavior of complexes **1–4** for the ROP of racemic α-MeTMC was examined and the results are summarized in Table 3. It can be found that all of these magnesium silylamido complexes can initiate effectively α-MeTMC polymerization in toluene at 70 °C, giving poly(α-MeTMC) with high molecular weights and relatively broad molecular weight distributions (M_w/M_n = 1.37–1.61).

The structure of the ancillary ligand also has a significant influence on the polymerization activity. Upon increasing the steric bulkiness of the ligand *ortho*-substituent, the catalytic activity of the corresponding magnesium complex apparently increases. Using complex **3** with an *ortho*-trityl group on the phenolate ring as the initiator, the monomer conversion can reach 92% within 60 min when adopting a monomer-to-initiator molar ratio of 200 (Run 5), whereas it is 90% when using complex **1** with an *ortho-tert*-butyl group after 180 min (Run 1). In contrast to the low efficiency displayed in *rac*-lactide polymerization in toluene, complex **4** with an *ortho*-bromo group exhibits a similar activity as complex **1**, although it is still less active (Runs 1, 2 *vs.* 7, 8).

To understand the difference between amide and alkoxide systems in initiation, α-MeTMC was polymerized with complexes **1–4** in the presence of 2-propanol. Similar to *rac*-LA polymerization carried out in toluene, the polymerizations by **1–4**/2-propanol are much faster and better controlled than those without 2-propanol. For example, using **1**/2-propanol as the initiator, the polymerization can reach 95% monomer conversion in 120 min and produce poly(α-MeTMC) with an average number molecular weight of 2.34×10^4 g mol^{-1}, which is very close to the theoretical value (2.20×10^4 g mol^{-1}, M_w/M_n = 1.37, Run 2).

To gain some insights into the polymerization of α-MeTMC with complexes **1–4**/2-propanol system, an NMR scale polymerization of α-MeTMC by complex **2** in the presence of 2-propanol was carried out. Treatment of complex **2** with one equiv. of 2-propanol, followed by addition of 20 equiv. of α-MeTMC in C_6D_6 at 30 °C revealed that, after 30 min, the *in situ* generated magnesium isopropoxide species initiate the ROP of α-MeTMC to give oligomers with an O^{i}Pr end group. The ^{1}H NMR spectrum of the purified oligomer clearly shows a set of resonances at δ 1.22 and 4.98 ppm assignable to the –OCH(CH$_3$)$_2$ end group (Fig. 3). The three signals at δ 4.36, 3.68, 1.28 ppm (labelled as a′, c′, and d′, respectively) can be assigned

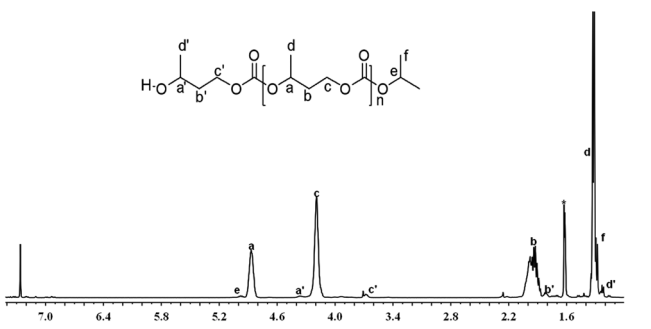

Fig. 3 ^{1}H NMR spectrum of α-MeTMC oligomers initiated by complex **2**/2-propanol ($[\alpha\text{-MeTMC}]_0 : [\mathbf{2}]_0 : [^i\text{PrOH}]_0$ = 20 : 1 : 1, 30 °C, $CDCl_3$).

Published on 17 January 2014. Downloaded by National Chung Hsing University on 02/04/2014 15:44:44.

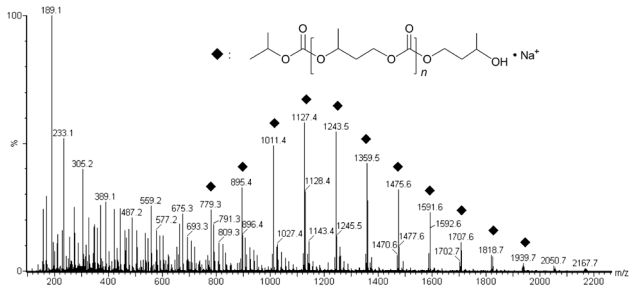

Fig. 4 ESI-TOF mass spectrum of α-MeTMC oligomers initiated by complex **2**/2-propanol ([α-MeTMC]$_0$: [**2**]$_0$: [^{i}PrOH]$_0$ = 20 : 1 : 1, 30 °C).

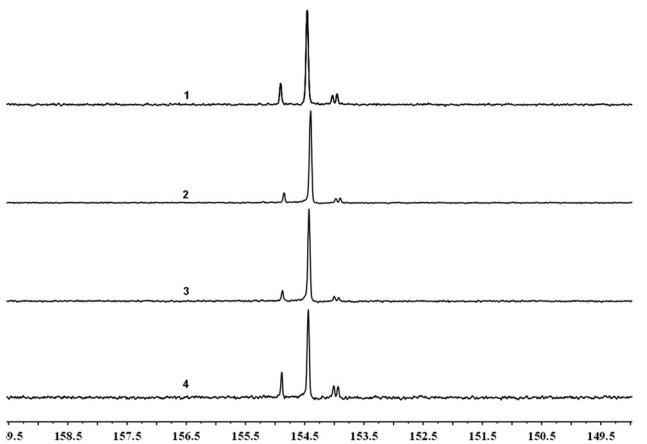

Fig. 5 Details of the carbonyl region of the $^{13}C\{^1H\}$ NMR spectra (100 MHz, $CDCl_3$, 25 °C) of poly(α-MeTMC): **1** (Table 3, Run 1) (X_{reg} = *ca.* 0.74), **2** (Table 3, Run 3) (X_{reg} = *ca.* 0.85), **3** (Table 3, Run 5) (X_{reg} = *ca.* 0.86), **4** (Table 3, run 7) (X_{reg} = *ca.* 0.65).

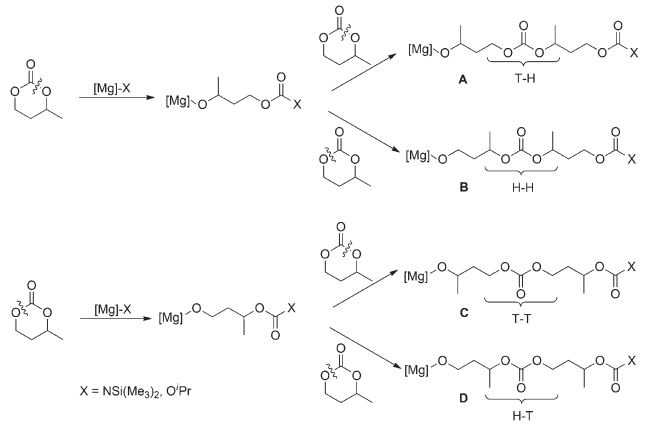

Scheme 3 Possible regioselective enchainments in the ROP of α-MeTMC.

respectively to the methine, methylene, and methyl groups of the other chain terminus.[57] Based on these features, the preferential ring-opening of α-MeTMC at the most hindered oxygen–acyl O–C(O) bond is therefore suggested. The ESI-TOF mass spectrum of the oligomer depicted in Fig. 4 also undoubtedly features one major distribution of peaks assigned to Na^+ ion cationized α-MeTMC oligomers terminated with hydroxyl and isopropoxy groups and with a repeat unit of 116 g mol^{-1} (*i.e.*, the molar mass of α-MeTMC).

Microstructure analyses of poly(α-MeTMC)s were further achieved through inspecting the carbonyl region of $^{13}C\{^1H\}$ NMR spectra of the resulting polymers (Fig. 5), since the resonances in this region are diagnostics of the diad sequences.[69] According to a literature report,[57] the biggest resonance at 154.4 ppm in the carbonyl region of the $^{13}C\{^1H\}$ NMR spectrum of poly(α-MeTMC) could be assigned to the indistinguishable diads **A** and **D** that are formed from the regioregular cleavage of either of the O–C(O) bonds in α-MeTMC (as depicted in Scheme 3). The other minor resonances at higher and lower fields (154.88, 154.01, 153.95 ppm) are representatives of those magnetically inequivalent carbonyl groups that result from the regioirregular enchainment of the monomer units, that is, from the alternated cleavage of different O–C(O) bonds in two sequential α-MeTMC molecules, denoted by diads **B** and **C**. By integrating these resonances in the carbonyl region of the $^{13}C\{^1H\}$ NMR spectra of poly(α-MeTMC) samples, it is clear that complexes **1–3** with a sterically bulky *ortho*-substituent on the phenolate ring are more regioselective in the polymerization (X_{reg} = 0.74 to 0.86) than complex **4** with an *ortho*-Br group, which displays a significantly lower regioselectivity of X_{reg} = 0.65. Furthermore, poly(α-MeTMC)s resulted by these complexes exhibit different thermal behaviour. The polymer sample obtained by complex **3** showed the characteristic thermal behavior of a T_g at −7.58 °C (Table 3, run 5) which is slightly higher than those reported in the literature (−18 to −10 °C).[56,57] The T_g values of other poly(α-MeTMC)s range around 4.32/4.01/1.43 °C (Table 3, runs 1, 3 and 7, respectively).

Conclusions

A series of racemic [ONN]-type iminophenols (**L^{1}H–L^{4}H**) based on the *N*-dimethylaminobiphenyl skeleton and their magnesium silylamido complexes have been synthesized and structurally characterized. X-Ray diffraction studies of typical complexes reveal that complex **1** is monomeric, but complex **4** with an *ortho*-bromo group on the phenoxide unit possesses a dimeric structure in the solid state. These magnesium silylamido complexes are efficient initiators for the ROP of *rac*-LA and α-MeTMC. The substituents of the ancillary ligand, especially the one at the *ortho*-position of the phenoxide ring of the ligand, have a profound influence on the catalytic activity and stereo-/region-selectivity. The most sterically hindered initiator **3** exhibits the highest activity and stereoselectivity from *rac*-LA polymerization (P_r = 0.81, −38 °C); meanwhile the same complex also shows the highest activity for ROP of α-MeTMC to afford highly regioregular polymers (X_{reg} = 0.86).

 This journal is © The Royal Society of Chemistry 2014

Published on 17 January 2014. Downloaded by National Chung Hsing University on 02/04/2014 15:44:44.

Experimental section

General considerations

All manipulations were carried out under a dry argon atmosphere using standard Schlenk-line or glove-box techniques. Toluene and *n*-hexane were refluxed over sodium benzophenone ketyl prior to use. Benzene-d_6, chloroform-*d* and other reagents were carefully dried and stored in the glove-box. $\{Mg[N(SiMe_3)_2]_2\}_2$,[70] 3-*tert*-butyl-2-hydroxy-5-methylbenzaldehyde,[71] 2-hydroxy-3,5-dicumylbenzaldehyde,[71] 5-*tert*-butyl-2-hydroxy-3-tritylbenzaldehyde,[72] and 5-*tert*-butyl-3-bromo-2-hydroxybenzaldehyde[73] were synthesized according to literature methods. Racemic-4-methyl-1,3-dioxan-2-one (α-MeTMC) was synthesized following literature procedures.[74] *rac*-Lactide (Aldrich) was recrystallized with dry toluene and then sublimed twice under vacuum at 80 °C. 2-Propanol was dried over calcium hydride prior to distillation. All other chemicals were commercially available and used after appropriate purification. Glassware and vials used in the polymerization were dried in an oven at 120 °C overnight and exposed to vacuum–argon cycle three times.

NMR spectra were recorded on a Bruker AVANCE-400 spectrometer at 25 °C (^{1}H: 400 MHz; ^{13}C: 100 MHz) unless otherwise stated. Chemical shifts for ^{1}H and ^{13}C NMR spectra were referenced internally using the residual solvent resonances and reported relative to tetramethylsilane (TMS). Elemental analyses were performed on an EA-1106 instrument. Spectroscopic analyses of polymers were performed in $CDCl_3$. Gel permeation chromatography (GPC) analyses were carried out on an Agilent instrument (L1200 pump, Optilab Rex injector) in THF at 25 °C at a flow rate of 1 mL min^{-1}. Calibration standards were commercially available narrowly distributed linear polystyrene samples that cover a broad range of molar masses ($10^3 < M_n < 2 \times 10^6$ g mol^{-1}). Differential scanning calorimetric (DSC) curves were taken on a Perkin–Elmer Pyris 1 instrument. All samples were cooled to −50 °C and heated to 100 °C for the first scan. After being kept for 1 min, they were again cooled to −50 °C and heated to 100 °C and then cooled to −50 °C for the second cycle. The heating rate was 10 °C min^{-1}.

Synthesis of the proligands and complexes

2-((2′-(Dimethylamino)biphenyl-2-ylimino)methyl)-4-methyl-6-*tert*-butylphenol (L^1H). 3-*tert*-Butyl-2-hydroxy-5-methylbenzaldehyde (0.961 g, 5.00 mmol) was mixed with 2-amino-2′-(dimethylamino)biphenyl (1.062 g, 5.000 mmol) in ethanol (50 mL). The mixture was refluxed at 80 °C and stirred for 5 h at this temperature. After being cooled to r.t., the solution was concentrated to about 20 mL and kept at −20 °C to afford yellow crystalline solids (1.546 g, 80%). Found: 386.2357. HRMS Calcd for $C_{26}H_{30}N_2O$: 386.2358; ^{1}H NMR ($CDCl_3$, 400 MHz, 298 K): δ 13.22 (s, 1H, O*H*), 8.36 (s, 1H, N–C*H*–Ar), 7.43 (d, 1H, J = 7.4 Hz, Ar*H*), 7.37 (t, 1H, J = 7.4 Hz, Ar*H*), 7.31 (t, 1H, J = 7.3 Hz, Ar*H*), 7.24 (m, 1H, Ar*H*), 7.16 (t, 2H, J = 7.4 Hz, Ar*H*), 7.09 (s, 1H, Ar*H*), 6.95 (m, 2H, Ar*H*), 6.89 (s, 1H, Ar*H*), 2.48 (s, 6H, $(CH_3)_2$N), 2.25 (s, 3H, C*H*$_3$–Ar), 1.35 (s, 9H, C$(CH_3)_3$). ^{13}C{^{1}H} NMR ($CDCl_3$, 100 MHz, 298 K): δ 162.6, 158.4, 151.4, 147.0, 137.2, 136.8, 132.1, 131.8, 131.0, 130.9, 130.0, 128.3, 128.0, 126.5, 126.4, 120.8, 118.8, 118.7, 117.4 (all Ar–*C*, N–*C*H–Ar), 43.1 ($(CH_3)_2$N), 34.7 ($C(CH_3)_3$), 29.2 (C$(CH_3)_3$), 20.6 (CH_3–Ar).

2-((2′-(Dimethylamino)biphenyl-2-ylimino)methyl)-4,6-dicumylphenol (L^2H). The procedure was the same as that of L^1H, except that 2-hydroxy-3,5-dicumylbenzaldehyde (1.792 g, 5.000 mmol) and amino-2′-(dimethylamino)biphenyl (1.062 g, 5.000 mmol) were used to afford L^2H as yellow crystalline solids (2.073 g, 75%). Found: 552.3143. HRMS Calcd for $C_{39}H_{40}N_2O$: 552.3141; ^{1}H NMR ($CDCl_3$, 298 K, 400 MHz): δ 12.91 (s, 1H, O*H*), 8.29 (s, 1H, N–*CH*–Ar), 7.37 (dd, 1H, J = 7.2 Hz, J = 1.7 Hz, Ar*H*), 7.32–7.27 (m, 6H, Ar*H*), 7.19 (m, 3H, Ar*H*), 7.17–7.08 (m, 6H, Ar*H*), 7.03 (dd, 1H, J = 7.4 Hz, J = 1.7 Hz, Ar*H*), 6.99 (d, 1H, J = 2.3 Hz, Ar*H*), 6.85 (t, 1H, J = 7.4 Hz, Ar*H*), 6.66 (d, 1H, J = 8.0 Hz, Ar*H*), 2.25 (s, 6H, $(CH_3)_2$N), 1.69 (s, 6H, C$(CH_3)_2$Ph), 1.59 (s, 6H, C$(CH_3)_2$Ph). ^{13}C{^{1}H} NMR ($CDCl_3$, 298 K, 100 MHz): δ 162.2, 157.6, 151.1, 150.8, 150. 6, 146.7, 139.3, 137.1, 136.3, 131.9, 130.7, 129.2, 128.2, 128.1, 128.0, 127.8, 127.6, 126.7, 126.5, 125.7, 125.6, 124.8, 120.4, 118.4, 117.3 (all Ar–*C*, N–*C*H–Ar), 42.8 ($(CH_3)_2$N), 42.4 ($C(CH_3)_2$Ph), 41.9 ($C(CH_3)_2$Ph), 30.89 (C$(CH_3)_2$Ph), 30.81 (C$(CH_3)_2$Ph).

2-((2′-(Dimethylamino)biphenyl-2-ylimino)methyl)-4-*tert*-butyl-6-tritylphenol (L^3H). The procedure was the same as that of L^1H, except that 5-*tert*-butyl-2-hydroxy-3-tritylbenzaldehyde (2.101 g, 5.000 mmol) and amino-2′-(dimethylamino)biphenyl (1.062 g, 5.000 mmol) were used to afford L^3H as yellow crystalline solids (2.580 g, 84%). Found: 614.3304. HRMS Calcd for $C_{44}H_{42}N_2O$: 614.3297; ^{1}H NMR ($CDCl_3$, 400 MHz, 298 K): δ 8.34 (s, 1H, N–*CH*–Ar), 7.37 (m, 2H, Ar*H*), 7.33 (dd, 1H, J = 7.6 Hz, J = 1.6 Hz, Ar*H*), 7.29 (dd, 1H, J = 7.3 Hz, J = 1.4 Hz, Ar*H*), 7.19 (br, 17H, Ar*H*), 7.09 (dd, 1H, J = 7.6 Hz, J = 1.6 Hz, Ar*H*), 7.02 (dd, 1H, J = 7.3 Hz, J = 1.4 Hz, Ar*H*), 7.09 (t, 1H, J = 7.4 Hz, Ar*H*), 6.64 (d, 1H, J = 8.2 Hz, Ar*H*), 2.19 (s, 6H, $(CH_3)_2$N), 1.18 (s, 9H, C$(CH_3)_3$). ^{13}C{^{1}H} NMR ($CDCl_3$, 100 MHz, 298 K): δ 162.6, 157.6, 150.9, 147.1, 145.5, 144.9, 139.6, 136.8, 134.0, 132.1, 131.8, 131.4, 131.0, 130.9, 130.6, 128.2, 127.8, 127.3, 127.2, 127.0, 126.4, 125.2, 120.5, 118.8, 118.5, 117.5 (all Ar–*C*, N–*C*H–Ar), 63.4 (Ar–*C*Ph$_3$), 42.9 ($(CH_3)_2$N), 34.0 ($C(CH_3)_3$), 31.3 (C$(CH_3)_3$).

2-((2′-(Dimethylamino)biphenyl-2-ylimino)methyl)-4-*tert*-butyl-6-bromophenol (L^4H). The procedure was the same as that of L^1H, except that 5-*tert*-butyl-3-bromo-2-hydroxybenzaldehyde (1.286 g, 5.000 mmol) and amino-2′-(dimethylamino)biphenyl (1.062 g, 5.000 mmol) were used to afford L^4H as orange crystalline solids (2.009 g, 89%). Found: 450.1309. HRMS Calcd for $C_{25}H_{27}BrN_2O$: 450.1307; ^{1}H NMR ($CDCl_3$, 400 MHz, 298 K): δ 13.31 (s, 1H, O*H*), 8.41 (s, 1H, N–C*H*–Ar), 7.57 (d, 1H, J = 2.4 Hz, Ar*H*), 7.45 (dd, 1H, J = 7.3 Hz, J = 1.6 Hz, Ar*H*), 7.40–7.34 (m, 2H, Ar*H*), 7.27 (m, 1H, Ar*H*), 7.22–7.13 (m, 3H, Ar*H*), 6.99 (m, 2H, Ar*H*), 2.47 (s, 6H, $(CH_3)_2$N), 1.29 (s, 9H, C$(CH_3)_3$). ^{13}C{^{1}H} NMR ($CDCl_3$, 100 MHz, 298 K): δ 161.8, 155.4, 151.3, 146.3, 142.4, 136.6, 133.3, 132.1, 131.4, 131.1, 128.5, 128.0, 127.8, 126.9, 121.0, 119.4, 119.0, 117.6, 110.5

Published on 17 January 2014. Downloaded by National Chung Hsing University on 02/04/2014 15:44:44.

(all Ar–*C*, N–*C*H–Ar), 43.1 ((*C*H$_3$)$_2$N), 34.0 (*C*(CH$_3$)$_3$), 31.3 (C(*C*H$_3$)$_3$).

[(L^1)MgN(SiMe$_3$)$_2$·THF] (1). The proligand **L^{1}H** (0.386 g, 1.00 mmol) was added slowly to a solution of {Mg[N(SiMe$_3$)$_2$]$_2$}$_2$ (0.345 g, 0.500 mmol) in toluene (20 mL). The solution was stirred for 24 h at r.t. All the volatiles were removed under vacuum. The resulting yellow solids were recrystallized with a mixture of THF and *n*-hexane at −38 °C to afford yellow crystals (321 mg, 50%). Found: C, 66.89; H, 8.46; N, 6.47. Anal. Calcd for $C_{36}H_{54}MgN_3O_2Si_2$: C, 67.42; H, 8.49; N, 6.55%; ^{1}H NMR (C_6D_6, 400 MHz, 298 K): δ 8.10 (s, 1H, N–*CH*–Ar), 7.30 (d, 1H, J = 2.4 Hz Ar*H*), 7.18 (m, 2H, Ar*H*), 7.12 (m, 2H, Ar*H*), 7.05 (td, 1H, J = 7.2 Hz, J = 1.4 Hz, Ar*H*), 6.93 (td, 1H, J = 8.2 Hz, J = 1.4 Hz, Ar*H*), 6.78 (t, 1H, J = 7.2 Hz, Ar*H*), 6.61 (m, 2H, Ar*H*), 3.34 (m, 4H, THF), 2.22 (s, 6H, (C*H*$_3$)$_2$N), 2.16 (s, 3H, C*H*$_3$–Ar), 1.60 (s, 9H, C(C*H*$_3$)$_3$), 1.20 (m, 4H, THF), 0.31 (s, 18H, N(Si(C*H*$_3$)$_3$)$_2$). ^{13}C{^{1}H} NMR (C_6D_6, 100 MHz, 298 K): δ 175.0, 168.6, 151.8, 150.4, 141.3, 135.4, 134.6, 134.3, 133.6, 133.0, 132.0, 128.84, 128.80, 126.6, 125.5, 122.2, 121.2, 120.0, 118.3 (all Ar–*C*, N–*C*H–Ar), 68.8 (THF), 44.0 (*C*H$_3$)$_2$N), 35.4 (*C*(CH$_3$)$_3$), 30.1 (C(*C*H$_3$)$_3$), 25.2 (THF), 20.8 (*C*H$_3$–Ar), 6.2 (N(Si-(*C*H$_3$)$_3$)$_2$).

[(L^2)MgN(SiMe$_3$)$_2$·toluene] (2). Following a procedure similar to that described for **1**, **L^{2}H** (0.553 g, 1.00 mmol) was treated with {Mg[N(SiMe$_3$)$_2$]$_2$}$_2$ (0.345 g, 0.500 mmol) in toluene (20 mL) at r.t. to give yellow solids. Recrystallization with a mixture of toluene and hexane at −38 °C afforded yellow crystalline solids (390 mg, 53%). Found: C, 75.21; H, 7.91; N, 5.06. Anal. Calcd for $C_{45}H_{57}MgN_3OSi_2·C_7H_8$: C, 75.38; H, 7.91;N, 5.07%; ^{1}H NMR (C_6D_6, 400 MHz, 298 K): δ 7.57 (s, 1H, N–*CH*–Ar), 7.49 (d, 1H, J = 2.7 Hz, Ar*H*), 7.25 (d, 2H, J = 7.2 Hz, Ar*H*), 7.19 (m, 5H, Ar*H*), 7.12–7.04 (m, 7H, Ar*H*), 7.00 (m, 4H, Ar*H*), 6.84 (m, 2H, Ar*H*), 6.75 (d, 1H, J = 2.7 Hz, Ar*H*), 6.60 (m, 2H, Ar*H*), 6.48 (d, 1H, J = 8.2 Hz, Ar*H*), 2.22 (s, 6H, (C*H*$_3$)$_2$N), 2.10 (s, 3H, C*H*$_3$ of toluene), 1.98 (s, 3H, C(C*H*$_3$)$_2$Ph), 1.54 (s, 6H, C(C*H*$_3$)$_2$Ph), 1.42 (s, 3H, C(C*H*$_3$)$_2$Ph), 0.26 (s, 18H, N(Si(C*H*$_3$)$_3$)$_2$). ^{13}C{^{1}H} NMR (C_6D_6, 100 MHz, 298 K): δ 172.5, 167.9, 152.5, 151.1, 149.1, 147.5, 141.0, 137.9, 136.1, 135.1, 134.3, 133.5, 13217, 131.9, 130.1, 129.5, 129.3, 128.5, 127.3, 127.1, 126.2, 125.8, 125.7, 125.4, 124.3, 123.9, 119.6, 119.3 (all Ar–*C*, N–*C*H–Ar), 46.2 (br, *C*H$_3$)$_2$N), 42.9 (*C*(CH$_3$)$_2$Ph), 42.4 (*C*(CH$_3$)$_2$Ph), 34.4 (C(*C*H$_3$)$_2$Ph), 31.1 (C(*C*H$_3$)$_2$Ph), 30.9 (C(*C*H$_3$)$_2$Ph), 26.5 (C(*C*H$_3$)$_2$Ph), 21.4 (*C*H$_3$–toluene), 7.4 (N(Si-(*C*H$_3$)$_3$)$_2$).

[(L^3)MgN(SiMe$_3$)$_2$·THF] (3). Following a procedure similar to that described for **1**, **L^{3}H** (0.615 g, 1.00 mmol) was treated with {Mg[N(SiMe$_3$)$_2$]$_2$}$_2$ (0.345 g, 0.500 mmol) in toluene (20 mL) at r.t. to give yellow solids. Recrystallization with a mixture of THF and hexane at −38 °C afforded yellow crystalline solids (444 mg, 51%). Found: C, 74.50; H, 7.84; N, 4.92. Anal. Calcd for $C_{54}H_{67}MgN_3O_2Si_2$: C, 74.50; H, 7.76; N, 4.83%; ^{1}H NMR (C_6D_6, 400 MHz, 298 K): δ 8.19 (s, 1H, N–*CH*–Ar), 7.63 (d, 1H, J = 2.6 Hz, Ar*H*), 7.43 (m, 6H, Ar*H*), 7.36 (d, 1H, J = 7.8 Hz, Ar*H*), 7.21 (t, 2H, J = 7.6 Hz, Ar*H*), 7.09 (br, 9H, Ar*H*), 6.98 (m, 3H, Ar*H*), 6.93 (d, 1H, J = 2.6 Hz, Ar*H*), 6.80 (t, 1H, J = 7.3 Hz, Ar*H*), 6.70 (d, 1H, J = 8.1 Hz, Ar*H*), 3.12 (m, 4H, THF), 2.23 (s, 6H, (C*H*$_3$)$_2$N), 1.17 (s, 9H, C(C*H*$_3$)$_3$), 1.15 (m, 4H THF), 0.09 (s, 18H, N(Si(C*H*$_3$)$_3$)$_2$). ^{13}C{^{1}H} NMR (C_6D_6, 100 MHz, 298 K): δ 174.4, 168.1, 151.6, 149.7, 147.1, 138.6, 135.9, 135.0, 134.4, 133.6, 132.9, 132.3, 131.9, 131.7, 128.8, 128.7, 127.4, 126.4, 126.0, 125.5, 122.4, 120.1, 118.4 (all Ar–*C*, N–*C*H–Ar), 68.4 ((CH$_2$*C*H$_2$)$_2$O), 64.1 (Ar–*C*Ph$_3$), 44.2 (*C*H$_3$)$_2$N), 33.9 (*C*(CH$_3$)$_3$), 31.5 (C(*C*H$_3$)$_3$), 24.9 ((*C*H$_2$CH$_2$)$_2$O), 6.1 (N(Si(*C*H$_3$)$_3$)$_2$).

[(L^4)MgN(SiMe$_3$)$_2$]$_2$ (4). Following a procedure similar to that described for **1**, **L^{4}H** (0.451 g, 1.00 mmol) was treated with {Mg[N(SiMe$_3$)$_2$]$_2$}$_2$ (0.345 g, 1.00 mmol) in toluene (20 mL) at r.t. to give yellow solids. Recrystallization with a mixture of toluene and hexane at −38 °C afforded yellow crystals (324 mg, 51%). Found: C, 58.19; H, 6.92; N, 6.27. Anal. Calcd for $C_{62}H_{88}Br_2Mg_2N_6O_2Si_4$: C, 58.63; H, 6.98; N, 6.62%; ^{1}H NMR of the major isomer (C_6D_6, 400 MHz, 298 K): δ 7.76 (d, 1H, J = 2.6 Hz, N–*CH*–Ar), 7.45 (s, 1H, Ar*H*), 7.08 (m, 1H, Ar*H*), 7.01 (m, 2H, Ar*H*), 6.70 (m, 4H, Ar*H*), 6.59 (d, 1H, J = 2.6 Hz, Ar*H*), 6.54 (d, 1H, J = 7.9 Hz, Ar*H*), 2.55 (s, 6H, (C*H*$_3$)$_2$N), 0.98 (s, 9H, Ar–C(C*H*$_3$)$_3$), 0.41 (s, 18H, N(Si(C*H*$_3$)$_3$)$_2$). ^{13}C{^{1}H} NMR of the major isomer (C_6D_6, 100 MHz, 298 K): δ 172.3, 164.4, 148.6, 147.5, 137.24, 137.21, 135.8, 134.4, 133.1, 130.9, 130.4, 129.4, 127.5, 127.2, 125.5, 123.7, 119.4, 118.7, 118.5 (all Ar–*C*, N–*C*H–Ar), 44.0 (*C*H$_3$)$_2$N), 33.9 (*C*(CH$_3$)$_3$), 31.1 (C(*C*H$_3$)$_3$), 6.9 (N(Si-(*C*H$_3$)$_3$)$_2$).

Typical procedure for the polymerization reaction

In a Braun Labstar glove-box, an initiator solution from a stock solution in THF or toluene was injected sequentially to a series of 10 mL vials loaded with *rac*-lactide or α-MeTMC and suitable amounts of dry solvent. After specified time intervals, each vial was taken out of the glove-box; an aliquot was withdrawn and quenched quickly with wet light petroleum ether, and the reaction mixture was quenched at the same time by adding an excess amount of light petroleum ether and one drop of water. All the volatiles in the aliquots were removed and the residue was subjected to monomer conversion determination which was monitored by integration of monomer *vs.* polymer methine or methyl resonances in ^{1}H NMR ($CDCl_3$, 400 MHz, 298 K). The precipitates collected from the bulk mixture were dried in air, dissolved with dichloromethane and sequentially precipitated into methanol. The obtained polymer was further dried in a vacuum oven at 50 °C for 16 h. Each reaction was used as one data point. In the cases where 2-propanol was used, the solution of the initiator was injected into the solution of the monomer in toluene to which 2-propanol was added. Otherwise the procedures were the same.

Oligomer preparation

Oligomerizations of *rac*-LA and α-MeTMC were carried out with complex **2**/2-propanol as the initiator in toluene, respectively, at 30 °C under the condition of a molar ratio of [Monomer]$_0$: [**2**]$_0$: [^{i}PrOH]$_0$ = 20 : 1 : 1. The reaction was stirred for 0.5 h and then quenched by adding wet hexane. The precipitated oligomers were collected, dried under vacuum, and used for ^{1}H NMR measurement or ESI-TOF.

 This journal is © The Royal Society of Chemistry 2014

Published on 17 January 2014. Downloaded by National Chung Hsing University on 02/04/2014 15:44:44.

X-ray crystallographic study

Suitable crystals of complexes **1** and **4** for X-ray analysis were obtained from a saturated solution of a tetrahydrofuran–pentane mixture or a toluene–pentane mixture, respectively, at −38 °C. Diffraction data were collected on a Bruker SMART APEX II diffractometer for complexes **1** and **4** with graphite-monochromated Mo Kα (λ = 0.71073 Å) radiation. All data were collected at 20 °C using the ϕ- and ω-scan techniques. All structures were solved by direct methods and refined using Fourier techniques. An absorption correction based on *SADABS* was applied.[75] All non-hydrogen atoms were refined by full-matrix least squares on F^2 using the *SHELXTL*[76] program package. Hydrogen atoms were located and refined by the geometry method. The cell refinement, data collection, and reduction were done using Bruker *SAINT*.[77] The structure solution and refinement were performed using *SHELXS-97*[78] and *SHELXL-2013* respectively. Molecular structures were generated using *ORTEP* program.[79]

Acknowledgements

This work was subsidized by the National Natural Science Foundation of China (NNSFC, 20604009, 21074032), the Program for New Century Excellent Talents in University (for H. Ma, NCET-06-0413) and the Fundamental Research Funds for the Central Universities (WD1113011, WK1214048). All the financial supports are gratefully acknowledged. H. Ma also acknowledges the very kind donation of a Braun glove-box by AvH Foundation.

Notes and references

1 A. J. Ragauskas, C. K. Williams, B. H. Davison and T. Tschaplinski, *Science*, 2006, **31**, 484–489.
2 C. K. Williams and M. A. Hillmyer, *Polym. Rev.*, 2008, **48**, 1–10.
3 S. Inkinen, M. Hakkarainen, A. C. Albertsson and A. Sodergard, *Biomacromolecules*, 2011, **12**, 523–532.
4 O. Dechy, B. Martin and D. Bourissou, *Chem. Rev.*, 2004, **104**, 6147–6176.
5 C. M. Thomas, *Chem. Soc. Rev.*, 2010, **39**, 165–173.
6 M. J. Stanford and A. P. Dove, *Chem. Soc. Rev.*, 2010, **39**, 486–494.
7 F. Qian, K. Liu and H. Ma, *Dalton Trans.*, 2010, **39**, 8071–8083.
8 A. D. Schwarz, Z. Chu and P. Mountford, *Organometallics*, 2010, **29**, 1246–1260.
9 C. Bakewell, R. H. Platel, S. K. Cary, S. M. Hubbard, J. M. Roaf, A. C. Levine, A. J. P. White, N. J. Long, M. Haaf and C. K. Williams, *Organometallics*, 2012, **31**, 4729–4736.
10 M. Lamberti, I. D'Auria, M. Mazzeo, S. Milione, V. Bertolasi and D. Pappalardo, *Organometallics*, 2012, **31**, 5551–5560.
11 G. Li, M. Lamberti, M. Mazzeo, D. Pappalardo, G. Roviello and C. Pellecchia, *Organometallics*, 2012, **31**, 1180–1188.
12 M. Normand, V. Dorcet, E. Kirillov and J.-F. Carpentier, *Organometallics*, 2013, **32**, 1694–1709.
13 A. Pietrangelo, S. C. Knight, A. K. Gupta, L. J. Yao, M. C. Hillmyer and W. B. Tolman, *J. Am. Chem. Soc.*, 2010, **132**, 11649–11657.
14 D. C. Aluthge, B. O. Patrick and P. Mehrkhodavandi, *Chem. Commun.*, 2012, **31**, 3499–3511.
15 L. B. Calvo, M. G. Davidson and D. García-Vivó, *Inorg. Chem.*, 2011, **50**, 3589–3595.
16 W.-Y. Lu, M.-W. Hsiao, S. C. N. Hsu, W.-T. Peng, Y.-J. Chang, Y.-C. Tsou, T.-Y. Wu, Y.-C. Lai, Y. Chen and H.-Y. Chen, *Dalton Trans.*, 2012, **41**, 3659–3667.
17 S. C. Roşca, D. A. Roşca, V. Dorcet, C. M. Kozak, F. Kerton, J.-F. Carpentier and Y. Sarazin, *Dalton Trans.*, 2013, **42**, 9361–9375.
18 R. K. Dean, A. M. Reckling, H. Chen, L. N. Dawe, C. M. Schneider and C. M. Kozak, *Dalton Trans.*, 2013, **42**, 3504–3520.
19 Y. Sarazin, B. Liu, T. Roisnel, L. Maron and J.-F. Carpentier, *J. Am. Chem. Soc.*, 2011, **133**, 9069–9087.
20 L. Wang and H. Ma, *Dalton Trans.*, 2010, **39**, 7897–7910.
21 S. Song, X. Zhang, H. Ma and Y. Yang, *Dalton Trans.*, 2012, **41**, 3266–3277.
22 I. D'Auria, M. Lamberti, M. Mazzeo, S. Milione, G. Roviello and C. Pellecchia, *Chem.–Eur. J.*, 2012, **18**, 2349–2360.
23 H. Wang and H. Ma, *Chem. Commun.*, 2013, **49**, 8686–8688.
24 S. Song, H. Ma and Y. Yang, *Dalton Trans.*, 2013, **42**, 14200–14211.
25 A. Garcés, L. F. Sánchez-Barba, C. Alonso-Moreno, M. Fajardo, J. Fernández-Baeza, A. Otero, A. Lara-Sánchez, I. López-Solera and A. M. Rodríguez, *Inorg. Chem.*, 2010, **49**, 2859–2871.
26 A. Grala, J. Ejfler, L. B. Jerzykiewicz and P. Sobota, *Dalton Trans.*, 2011, **40**, 4042–4044.
27 L. Wang and H. Ma, *Macromolecules*, 2010, **43**, 6535–6537.
28 H.-Y. Chen, L. Mialon, K. A. Abboud and S. A. Miller, *Organometallics*, 2012, **31**, 5252–5261.
29 Y. Wang, W. Zhao, D. Liu, S. Li, X. Liu, D. Cui and X. Chen, *Organometallics*, 2012, **31**, 4182–4190.
30 J. P. Davin, J.-C. Buffet, T. P. Spaniol and J. Okuda, *Dalton Trans.*, 2012, **41**, 12612–12618.
31 B. Liu, T. Roisnel, J.-P. Guégan, J.-F. Carpentier and Y. Sarazin, *Chem.–Eur. J.*, 2012, **18**, 6289–6301.
32 E. L. Whitelaw, M. D. Davidson and M. D. Jones, *Chem. Commun.*, 2011, **47**, 10004–10006.
33 A. Sauer, J.-C. Buffet, T. P. Spaniol, H. Nagae, K. Mashima and J. Okuda, *Inorg. Chem.*, 2012, **51**, 5764–5770.
34 A. Stopper, J. Okuda and M. Kol, *Macromolecules*, 2012, **45**, 698–704.
35 C.-Y. Li, C.-J. Yu and B.-T. Ko, *Organometallics*, 2013, **32**, 172–180.
36 H. Ma, T. P. Spaniol and J. Okuda, *Dalton Trans.*, 2003, 4770–4780.
37 S. Yang, D. Zhu, Y. Zhang and Q. Shen, *Chem. Commun.*, 2012, **48**, 9780–9782.

Published on 17 January 2014. Downloaded by National Chung Hsing University on 02/04/2014 15:44:44.

38 C. Bakewell, T.-P.-A. Cao, N. Long, X. F. L. Goff, A. Auffrant and C. K. Williams, *J. Am. Chem. Soc.*, 2012, **134**, 20577–20580.
39 J. Kratsch, M. Kuzdrowska, M. Schmid, N. Kazeminejad, C. Kaub, P. Oña-Burgos, S. M. Guillaume and P. W. Roesky, *Organometallics*, 2013, **32**, 1230–1238.
40 K. Nie, W. Gu, Y. Yao, Y. Zhang and Q. Shen, *Organometallics*, 2013, **32**, 2608–2617.
41 B. Calvo, M. G. Davidson and D. García-Vivó, *Inorg. Chem.*, 2011, **50**, 3589–3595.
42 W.-Y. Lu, M.-W. Hsiao, S. C. N. Hsu, W.-T. Peng, Y.-J. Chang, Y.-C. Tsou, T.-Y. Wu, Y.-C. Lai, Y. Chen and H.-Y. Chen, *Dalton Trans.*, 2012, **41**, 3659–3667.
43 B. M. Chamberlain, M. Cheng, D. R. Moore, T. M. Ovitt, E. B. Lobkovsky and G. W. Coates, *J. Am. Chem. Soc.*, 2001, **123**, 3229–3238.
44 M. Chisholm, J. Huffman and K. Phomphrai, *J. Chem. Soc., Dalton Trans.*, 2001, 222–224.
45 M. Chisholm and K. Phomphrai, *Inorg. Chim. Acta*, 2003, **350**, 121–125.
46 A. Dove, V. Gibson, E. Marshall, A. White and D. Williams, *Dalton Trans.*, 2004, 570–578.
47 H.-Y. Chen, H.-Y. Tang and C.-C. Lin, *Macromolecules*, 2006, **39**, 3745–3752.
48 D. J. Darensbourg and O. Karroonnirun, *Inorg. Chem.*, 2010, **49**, 2360–2371.
49 K. Makiguchi, Y. Ogasawara, S. Kikuchi, T. Satoh and T. Kakuchi, *Macromolecules*, 2013, **46**, 1772–1782.
50 B. Liu, T. Roisnel, L. Maron, J.-F. Carpentier and Y. Sarazin, *Chem.–Eur. J.*, 2013, **19**, 3986–3994.
51 F. Hild, N. Neehaul, F. Bier, M. Wirsum, C. Gourlaouen and S. Dagorne, *Organometallics*, 2013, **32**, 587–598.
52 H. Sheng, J. Shi, Y. Feng, H. Wang, Y. Jiao, H. Sheng, Y. Zhang and Q. Shen, *Dalton Trans.*, 2012, **41**, 9232–9240.
53 P. Brignou, S. M. Guillaume, T. Roisnel, D. Bourissou and J.-F. Carpentier, *Chem.–Eur. J.*, 2012, **18**, 9360–9370.
54 V. Poirier, T. Roisnel, S. Sinbandhit, M. Bochmann, J.-F. Carpentier and Y. Sarazin, *Chem.–Eur. J.*, 2012, **18**, 2998–3013.
55 D. J. Darensbourg, O. Karroonnirun and S. J. Wilson, *Inorg. Chem.*, 2011, **50**(14), 6775–6787.
56 J. Ling, Y. Dai, Y. Zhu, W. Sun and Z. Shen, *J. Polym. Sci., Part A: Polym. Chem.*, 2010, **48**, 3807–3815.
57 P. Brignou, J.-F. Carpentier and S. M. Guillaume, *Macromolecules*, 2011, **44**, 5127–5135.
58 W. Yi and H. Ma, *Inorg. Chem.*, 2013, **52**, 11821–11835.
59 W. L. Mosby, *J. Org. Chem.*, 1957, **22**, 671–673.
60 D. Purdie, *J. Am. Chem. Soc.*, 1941, **63**, 2276.
61 H.-Y. Tang, H.-Y. Chen, J.-H. Huang and C.-C. Lin, *Macromolecules*, 2007, **40**, 8855–8860.
62 H. Ma and J. Okuda, *Macromolecules*, 2005, **38**, 2665–2673.
63 W.-C. Hung and C.-C. Lin, *Inorg. Chem.*, 2009, **48**, 728–734.
64 Y. Wang and H. Ma, *Chem. Commun.*, 2012, **48**, 6729–6731.
65 L. M. Alcazar-Roman, B. J. O'Keefe, M. A. Hillmyer and W. B. Tolman, *Dalton Trans.*, 2003, 3082–3087.
66 H. Ma, T. P. Spaniol and J. Okuda, *Angew. Chem., Int. Ed.*, 2006, **45**, 7818–7821.
67 M. H. Chisholm, K. Choojun, J. C. Gallucci and P. M. Wambua, *Chem. Sci.*, 2012, **3**, 3445–3457.
68 A. Amgoune, C. M. Thomas, T. Roisnel and J.-F. Carpentier, *Chem.–Eur. J.*, 2006, **12**, 169–179.
69 P. Brignou, G. M. Priebe, O. Casagrande, J.-F. Carpentier and S. M. Guillaume, *Macromolecules*, 2010, **43**, 8007–8017.
70 M. Westerhausen, *Inorg. Chem.*, 1991, **30**, 96–101.
71 G. Casiraghi, G. Casnati, G. Puglia, G. Sartori and G. Terenghi, *J. Chem. Soc., Perkin Trans. 1*, 1980, 1862–1865.
72 A. I. Kochnev, I. I. Oleynik, I. V. Oleynik, S. S. Ivanchev and G. A. Tolstikov, *Russ. Chem. Bull., Int. Ed.*, 2007, **56**, 1125–1129.
73 F. Lam, J. Xu and K. Chan, *J. Org. Chem.*, 1996, **61**, 8414–8418.
74 H. Yasuda, M.-S. Aludin, N. Kitamura, M. Tanabe and H. Sirahama, *Macromolecules*, 1999, **32**, 6047–6057.
75 SADABS, *Bruker Nonius area detector scaling and absorption correction, version 2.05*, Bruker AXS Inc., Madison, WI, 1996.
76 G. M. Sheldrick, *SHELXTL 5.10 for windows NT, Structure Determination Software Programs*, Bruker AXS Inc., Madison, WI, 1997.
77 *SAINT, version 6.02*, Bruker AXS Inc., Madison, WI, 1999, pp. 53711–55373.
78 G. M. Sheldrick, *SHELXS-97, Program for the Solution of Crystal Structures*, University of Göttingen, Göttingen, Germany, 1990.
79 L. J. Farrugia, ORTEP-III for Windows, version 2.0, *J. Appl. Crystallogr.*, 1997, **30**, 565.

 This journal is © The Royal Society of Chemistry 2014